energy&fuels

Article

pubs.acs.org/EF

Density Functional Theory Study of the Concerted Pyrolysis Mechanism for Lignin Models

Thomas Elder*,[†] and Ariana Beste[‡]

[†]Southern Research Station, United States Department of Agriculture (USDA) Forest Service, Pineville, Louisiana 71360, United States

[‡]Joint Institute for Computational Sciences, The University of Tennessee, Knoxville, Tennessee 37996, United States

Supporting Information

ABSTRACT: Studies on the pyrolysis mechanisms of lignin model compounds have largely focused on initial homolytic cleavage reactions. It has been noted, however, that concerted mechanisms may also account for observed product formation. In the current work, the latter processes are examined and compared to the former, by the application of density functional theory calculations to fully substituted lignin models. Results show that activation energies for the concerted reactions are somewhat lower than the bond dissociation energies of the homolysis reactions. Kinetic analysis revealed that the concerted pathway is the retro-ene fragmentation mechanism.

INTRODUCTION

Political and economic uncertainty along with concerns regarding environmental and sustainability issues have resulted in considerable recent interest in the use of renewable materials for fuels and chemicals currently derived from fossil sources. Lignocellulosic biomass can be processed for such applications through biochemical or thermochemical methods or combinations thereof in the biorefinery concept.[1,2] An integral part of the latter is the thermal degradation of lignin.[3,4]

The lignin polymer is derived from free radicals produced by the enzymatic dehydrogenation of the cinnamyl alcohols. These radicals can exist in a number of resonance forms, accounting for the variety of interunit linkages present in the polymer. Among these, the most frequent is the β−O−4 bond, which is responsible for 50−60% of the linkages. Given the preponderance of this bond type, it is of major importance in the chemistry of lignin in general and pyrolysis in particular. Information on the fundamental chemistry of these reactions may be of utility in their control and, therefore, the products that are generated. To this end, the mechanisms associated with lignin pyrolysis and especially β−O−4 dimers have been the topic of both experimental and computational research.

As part of a substantial body of experimental work reported by Kawamoto and co-workers,[5−7] the pyrolysis of guaicyl-based β−O−4 models was found to be profoundly affected by the presence of a phenolic group, markedly increasing the reactivity, resulting in coniferyl alcohol and guaiacol as the major products.[8] Working with similar compounds at relatively low temperatures and on the basis of the presence of guaiacol in the reaction mixtures, the first step is proposed to be the cleavage of the ether bond.[9] Under hydrodeoxygenation conditions, in the presence of ethanol at 380 °C, initial homolytic cleavage of the β−O bond with subsequent free radical reactions is proposed, whereas the addition of an α−OH group results in products indicative of C_α−C_β cleavage.[10] Two recent papers have examined the pyrolysis of β−O−4 oligomers using thermogravimetric analysis and pyrolysis gas chromatography−mass spectrometry (GC−MS), among other instrumental methods.[11,12] As in the previous work, the main reactions appear to involve the β−O and C_α−C_β bonds. This is also consistent with results from thermogravimetric analysis on dilignols.[13] In work on variously substituted phenethyl phenyl ethers, representing the ubiquitous β−O−4 linkage in lignin, Britt and co-workers have invoked a free radical chain reaction initiated by homolytic cleavage to account for the products.[14,15] In the former paper, however, it is discussed that styrene and phenol from the degradation of phenethyl phenyl ether could also arise from a concerted 1,2 elimination reaction, when experimental conditions suppress the occurrence of bimolecular reactions. Deuterium isotope effect experiments reveal a preference for the homolytic cleavage reaction, but it is discussed that the concerted reaction could occur at low pressures. Indeed, in earlier work, kinetics predicted from concerted mechanisms identified as the Maccoll elimination and retro-ene fragmentation corresponded most closely with the experimental results.[16] Using photoionization time-of-flight mass spectrometry to analyze the products from the pyrolysis of phenethyl phenyl ether in a hyperthermal nozzle in conjunction with CBS-QB3 calculations, it was reported that the concerted mechanisms dominate at temperatures below 1000 °C.[17] Similar results were found in a computational study at the B3LYP/6-31G(d) level of theory.[18] On the basis of the proposed homolytic cleavage reactions, there have been several computational studies examining bond dissociation enthalpies of lignin models[19−28] and kinetic work primarily based on phenethyl phenyl ether models.[29−35] Finally, on the basis of kinetic analyses, an experimental method is described for elucidating whether the free radical or concerted mechanism is occurring in pyrolysis.[36]

Received: June 18, 2014
Revised: July 18, 2014
Published: July 20, 2014

ACS Publications © 2014 American Chemical Society

dx.doi.org/10.1021/ef5013648 | *Energy Fuels* 2014, 28, 5229−5235

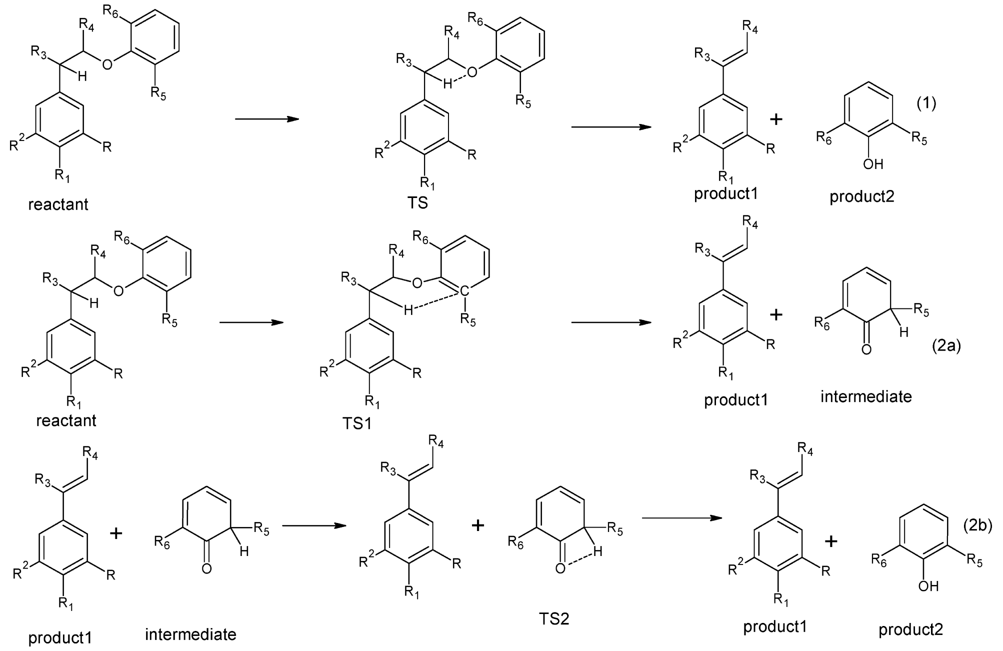

Figure 1. Concerted reactions for the lignin models.

Given the work of Jarvis et al.[17] and Huang et al.[18] comparing the homolytic cleavage and concerted reactions of phenethyl phenyl ether, the objective of the current paper is to examine these processes for completely substituted β–O–4 lignin models by the application of density functional theory calculations.

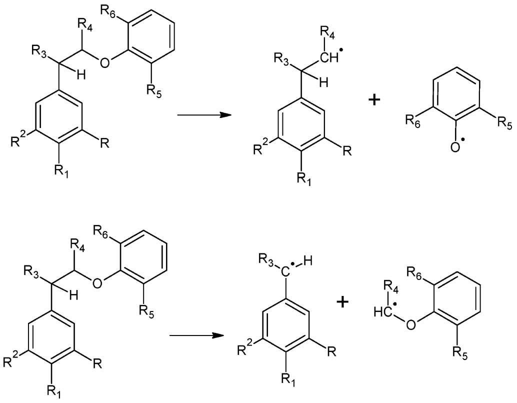

Figure 2. Homolytic cleavage reactions for the lignin models.

■ EXPERIMENTAL SECTION

The structures and reactions evaluated are as shown in Figure 1, where eq 1 corresponds to the Maccoll elimination and eqs 2a and 2b are the retro-ene fragmentation. The reactants represent guaiacyl (G) (R_2 and R_6 = H, R and R_5 = OCH_3, R_1 and R_3 = OH, and R_4 = CH_2OH), syringyl (S) (R, R_2, R_5, and R_6 = OCH_3, R_1 and R_3 = OH, and R_4 = CH_2OH), and *para*-hydroxy (H) (R, R_2, R_5, and R_6 = H, R_1 and R_3 = OH, and R_4 = CH_2OH) models, with phenethyl phenyl ether (PPE) (R, R_1, R_2, R_3, R_4, R_5, and R_6 = H) included for comparison purposes. Because of the asymmetric substitution of the guaicyl model, in the course of the retro-ene fragmentation, the α hydrogen can attack either the 3′ carbon with a methoxy group or the 5′ carbon, bearing hydrogen. Both possibilities were evaluated, such that, for G(1), R_2 and R_6 = H, R and R_5 = OCH_3, R_1 and R_3 = OH, and R_4 = CH_2OH and for G(2), R_2 and R_5 = H, R and R_6 = OCH_3, R_1 and R_3 = OH, and R_4 = CH_2OH. In addition, the energetics of the homolytic cleavage reactions (Figure 2) were determined, in which the reactants were modeled as singlets and products were modeled as doublets. While these have been previously reported in the literature,[19−24] they are repeated here, using consistent computational methods, to ensure comparability. A crystal structure has been reported for the guaiacyl reactant,[37] which was used as the basis for all of the reactants in the current work.

All calculations were performed using Gaussian 09, Revision C.01,[38] as implemented on the Dense Memory Cluster on the Alabama Supercomputer Network. Density functional calculations were performed using the M06-2X method[39] and the 6-311++G(d,p) basis set with full geometry optimization and frequency calculations, assuming the harmonic oscillator approximation and thermal corrections at 873 K, using the ultrafine integration grid with 99 radial shells and 590 angular points per shell. Charges were determined using the natural bond order method. On the basis of energy calculations on a test set of compounds, the M06-2X method was found to have a mean unsigned error of 1.3 kcal mol^{-1}.[39] Transition states were confirmed by the identification of a single imaginary frequency and intrinsic reaction coordinate calculations. The zero-point-corrected reaction energies for each step are based on the difference between products and reactants for each step.

Rate constants for each elementary step were calculated as $k = (k_BT/h)\exp(-\Delta G/RT)$, where k_B is Boltzmann's constant, T is the temperature in kelvin, h is Planck's constant, R is the gas constant, and ΔG is Gibbs free energy of activation at 600 °C. It can be seen that, for the purposes of the current work, the transmission coefficient (κ), representing reflection or tunneling of the transition state, is neglected. This is based on previous literature that addresses the uncertainties associated with the calculation of this term[40,41] and the accuracy of ΔG, which can result in variability greater than the correction associated with the inclusion of the transmission coefficient.[42] Using Mathematica, these values were then used in kinetic simulations to follow product formation and substrate depletion as a function of time. The simulations assumed an initial substrate concentration of 1×10^{-8} mol L^{-1} and a temperature of 600 °C, consistent with experimental conditions reported in the literature, in which the occurrence of concerted reactions was postulated.[14] While the two proposed concerted mechanisms result in the same products, they were simulated separately to analyze pathway contributions. In addition, the validity of using the steady-state approximation for the series of elementary steps in the retro-ene pathway was evaluated.

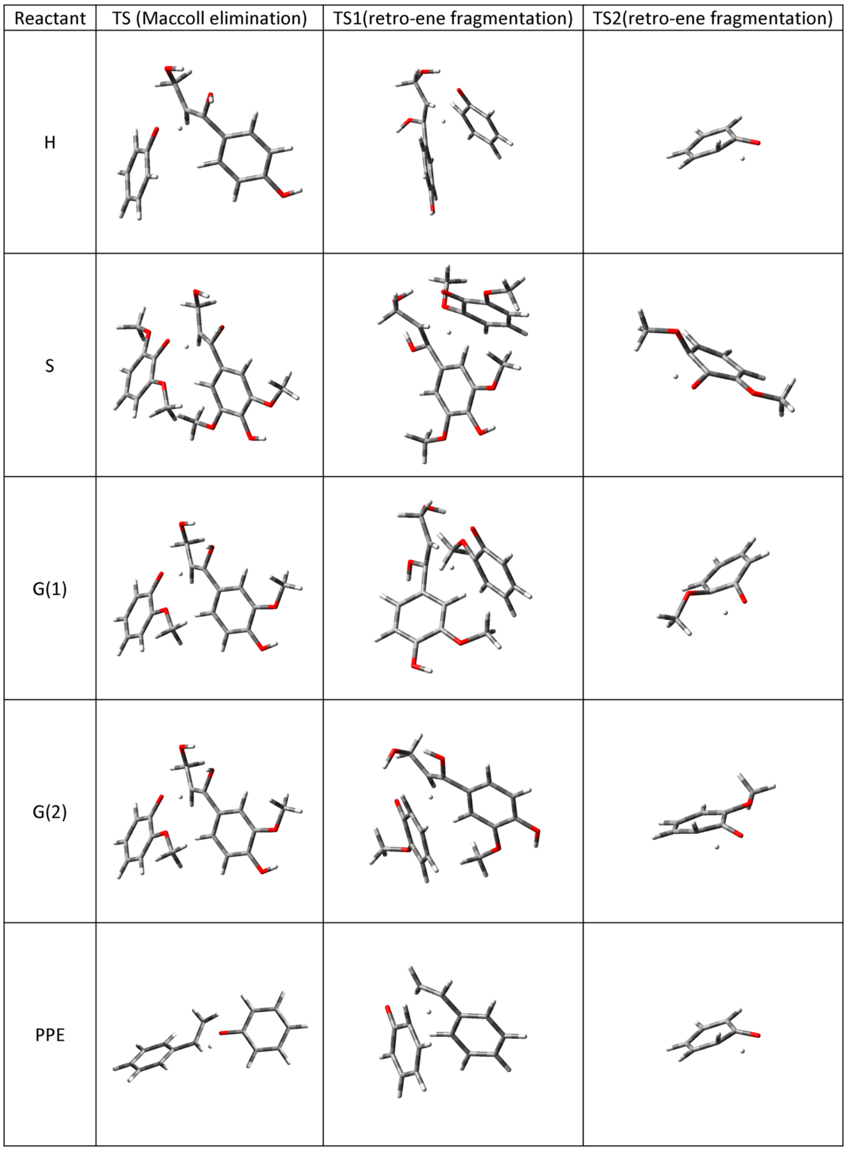

Figure 3. Geometry for the transition states for the lignin models.

■ RESULTS AND DISCUSSION

The geometry for the transition states arising from each substrate is as shown in Figure 3. The zero-point-corrected energies in kcal mol^{-1}, relative to the energy of the initial reactant, for the Maccoll elimination mechanism and retro-ene fragmentation are as shown in Figure 4. For calibration purposes, it can be seen that the results for phenethyl phenyl ether are consistent with those previously reported.[18] The variations observed may be due to the use of a different functional (M06-2X in the current work and B3LYP in ref 18) and larger basis set [6-311++G(d,p) in the current work and 6-31G(d) in ref 18] and/or differences in geometry.

The activation energies for the transition states of the Maccoll elimination mechanism are all reasonably similar, with phenethyl phenyl ether exhibiting the lowest barrier. Among the substituted lignin models, the activation energies are in the range of ~65−66 kcal mol^{-1}, with the syringyl structure having a slightly lower value. The overall reaction to the phenolic and styrene products is uniformly endothermic from 12.66 to 15.99 kcal mol^{-1}, the highest of which is the syringyl model. The variability in energies notwithstanding, given the reported accuracy (1.3 kcal mol^{-1}) of the M06-2X functional,[39] are quite similar and do not represent significant differences.

The first step in the retro-ene fragmentation is found to have lower activation energies, in agreement with the previous literature.[17,18] For PPE, the difference between the two mechanisms is found to be 7.36 kcal mol^{-1}, in excellent agreement with the 7.3 value previously reported.[18] Furthermore, this initial barrier is more variable among the substituted lignin models, the highest of which is the G(1) transition state, in which the reaction involves the methoxy-substituted position, while the lowest is the G(2) transition state, reacting through an unsubstituted aromatic carbon. The *para*-hydroxy (H) and syringyl (S) models are intermediate, with syringyl interestingly being the lower of the two. While steric arguments could legitimately be made to account for the observed energetic differences, electronic factors within the reactants may also be of importance, because a negative charge at the reactive carbon would facilitate electrophilic attack. In this regard, the natural bond orbital (NBO) charges at the unsubstituted aromatic positions are −0.30, −0.27, and −0.23 for PPE, H, and G, respectively, all of which exhibit low activation energy

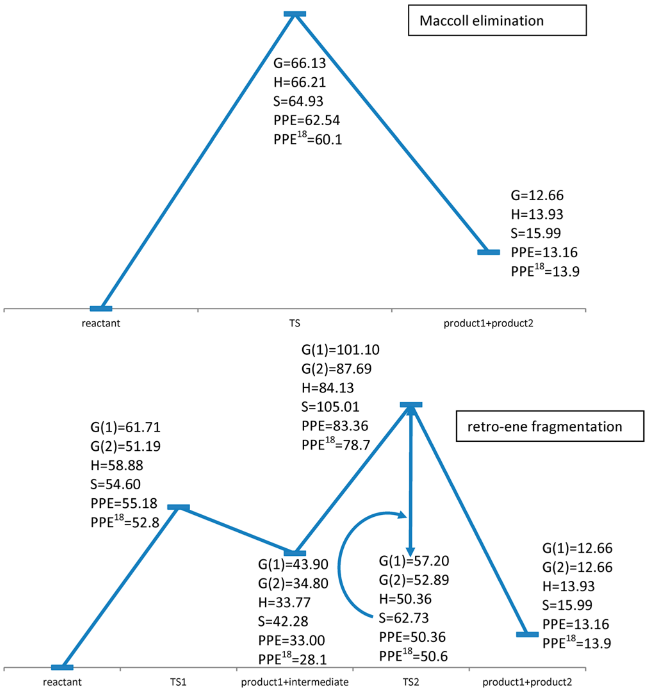

Figure 4. Reaction profiles for the Maccoll elimination and retro-ene fragmentation mechanisms.

Table 1. Zero-Point-Corrected Bond Dissociation Energies (kcal mol^{-1}) for β−O and α−β Homolytic Cleavage for the Lignin Models

	bond cleavage reaction	
reactant	β−O	α−β
G	68.81	75.19
H	70.83	74.34
S	68.32	79.35
PPE	69.34	76.59

barriers. With methoxylation, however, electrons are withdrawn, and this position for the S and G models has partial positive charges of 0.31 and 0.29, respectively. This translates into a high activation energy for the G(1) transition state but a remarkably low barrier for the syringyl model. The latter may be rationalized as an effect of the presence of an *ortho*-methoxy group that does not participate in the reaction. This is supported by the results for the G(2) transition state, for which the activation energy is lower than the H and PPE models, despite a somewhat increased steric hindrance and a smaller partial negative charge. The presence of an *ortho*-methoxy group has been recently discussed in the context of bond dissociation enthalpies[22] and acid-catalyzed depolymerization of lignin.[43] The results from the latter showed that, because of its electron-withdrawing nature, an *ortho*-methoxy group deactivated the ring toward electrophilic aromatic substitution and reduced resonance stabilization, while the former showed changes in aromaticity with substitution. In light of these interpretations, while regardless of the transition state, the *ortho*-methoxy group in the G reactant will deactivate the ring, the G(2) structure may retain some resonance stabilization, as evidenced by increased aromaticity, resulting in the lowered activation energy barrier.

The products resulting from this first transition state are all endothermic with respect to the initial reactants. The energies for these structures are consistent with substitution, such that G(1) involving the reaction at the methoxylated position is similar to the syringyl products, while G(2), PPE, and H products that have reacted through an unsubstituted site are similar. Tautomerization of the quinone intermediates to the phenolic products proceeds through TS2, with activation energies ranging from about 50 to 62 kcal mol^{-1}. Within these, the lowest barriers again occur in the structures that have been hydrogenated at non-methoxy sites. It is recognized that the Maccoll elimination mechanism and the proposed four-membered transition state may be of concern sterically and energetically. Furthermore, for the dilgnol models with γ−OH groups, alternative routes may be available for the thermal degradation of such compounds. The rationale for limiting the current work to the Maccoll elimination and retro-ene fragmentation is their proposal in the literature[14−18,36] and ability to account for the experimentally observed products from phenethyl phenyl ether pyrolysis.

For comparison purposes, the zero-point-corrected energies for the homolytic cleavage reactions are as shown in Table 1. These homolytic cleavage reactions have been proposed to be barrierless, and as such, the activation energies can be approximated by the reaction energy.[17,25] As previously reported, the C−C bond dissociation energies are greater than the β−O values. All of these energies are higher than the reaction barriers for the concerted mechanisms, such that, in a

Table 2. Gibbs Free Energy of Activation (kcal mol^{-1}) and Rate Constants (s^{-1}) for the Mechanisms and Lignin Models

Maccoll elimination			G		H	S	PPE
forward		ΔG_{600}	67.72		63.68	64.5	62.01
		k	2.04×10^{-4}		2.09×10^{-3}	1.31×10^{-3}	5.48×10^{-3}
reverse		ΔG_{600}	104.9		91.06	92.12	79.85
		k	1.01×10^{-13}		2.94×10^{-10}	1.59×10^{-10}	1.88×10^{-7}
retro-ene fragmentation			G(1)	G(2)	H	S	PPE
reaction 1	forward	ΔG_{600}	66.21	55.86	58.36	57.18	58.49
		k	4.87×10^{-4}	1.90×10^{-1}	4.49×10^{-2}	8.87×10^{-2}	4.17×10^{-2}
	reverse	ΔG_{600}	74.75	73.08	69.66	58.9	60.24
		k	3.55×10^{-6}	9.30×10^{-6}	6.67×10^{-5}	3.29×10^{-2}	1.52×10^{-2}
reaction 2	forward	ΔG_{600}	58.28	55.74	55.07	62.23	55.07
		k	4.71×10^{-2}	2.03×10^{-1}	2.99×10^{-1}	4.83×10^{-3}	2.99×10^{-1}
	reverse	ΔG_{600}	86.91	74.69	71.16	88.12	71.16
		k	3.21×10^{-9}	3.68×10^{-6}	2.81×10^{-5}	1.60×10^{-9}	2.81×10^{-5}

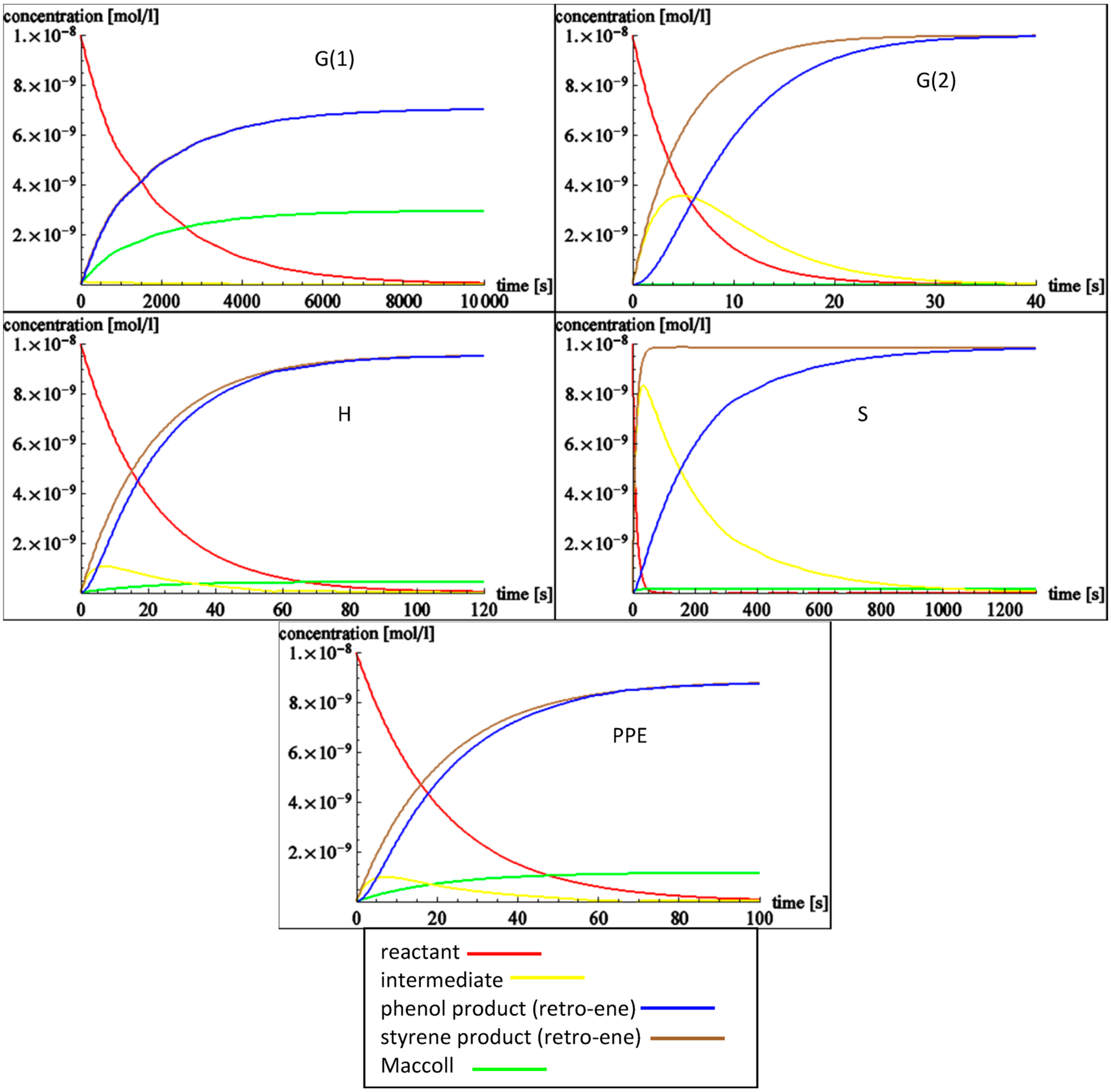

Figure 5. Concentration of reactant, intermediate, and products as a function of time, at 873 K.

regime favorable to the unimolecular reactions, the concerted mechanisms would be dominant.

Because the retro-ene fragmentation proceeds through an intermediate, the barriers for the retro-ene and the Maccoll reaction are not directly comparable. As such, kinetic simulations were performed at experimental conditions[14] to understand pathway selectivity. The Gibbs free energy of activation and rate constants used in the kinetics simulation are given in Table 2, and the graphical results from the kinetics simulations are as shown in Figure 5. G(1) and G(2) represent the two distinct pathways for retro-ene fragmentation of the guaiacyl model (G) that are in competition. The G(1) pathway has a negligible contribution to the conversion of G via retro-ene fragmentation but is given as a separate graph to show substituent influence. It can be seen that, for all investigated model compounds, the retro-ene pathway dominates over the Maccoll elimination. The lower barriers for the first transition of the retro-ene pathway found for PPE, H, and G(2) correspond to rapid conversion in comparison to G(1) and S. As pointed out previously, methoxy substitution at the reactive carbon center destabilizes the transition state for the latter models, but this is counteracted by the stabilizing effect of the *ortho*-methoxy substituent not associated with the reactive center. This is reflected in the faster conversion rate of S than G(1), while G(2) reacts faster than H and PPE. In fact, conversion of G through the G(1) retro-ene pathway becomes so slow that the Maccoll reaction is competitive, exhibiting a retro-ene/Maccoll selectivity at steady state of 2.4. However, because the retro-ene product is almost exclusively formed through the G(2) pathway, Figure 5 shows that concerted product formation of substituted β–O–4 model compounds proceeds largely (selectivity of 22 at steady state for H) to almost exclusively (S and G) via the retro-ene fragmentation. The Maccoll reaction has a higher contribution to PPE conversion with a calculated selectivity of 7.6 at steady-state conditions.

The steady-state approximation for a series of reactions that proceed via an intermediate is often useful because it results in an overall rate constant. The approximation involves setting the rate of change of the intermediate equal to zero, which can be rationalized if the barrier from intermediate to product is small. Because this is not the case here, the steady-state approximation was not applied *a priori*. Figure 5 shows that [with the exception of G(1)] the phenolic product from the retro-ene mechanism is formed somewhat more slowly than the styrene or styrene analogue. This is mirrored in the concentration of the intermediate that is initially non-zero, proceeds through a maximum, and tends to zero at steady-state conditions. The Supporting Information contains the kinetic simulation results of the retro-ene fragmentation of G(1), G(2), S, H, and PPE, which are compared to product formation when the steady-state approximation is applied. For G(1), the steady-state approximation is applicable through the entire reaction time. For H and G(2), the steady-state concentration follows the phenolic product concentration of the full simulation, yielding identical product distribution steady-state conditions. This is similar for PPE with a slight underestimation of product concentration at steady-state conditions when the steady-state approximation is invoked. In contrast, the steady-state approximation for S fails even at steady-state conditions. It can be seen in Figure 5 that, for S, the intermediate accumulates up to a high concentration before the second step of the retro-ene mechanism takes place. This is consistent with the fact that, for S, the second free energy barrier is higher than the first (Table 2).

The current work represents the first computational examination of the proposed concerted pyrolysis mechanism for fully substituted lignin models. In general, the results are in agreement with previous literature reporting analogous reactions of phenethyl phenyl ether.[17,18] Activation energies of the substituted models are somewhat higher than PPE. The activation energy barriers for both of the mechanisms under consideration are lower than the bond dissociation energies associated with homolytic cleavage, but the latter is only the initial step in a chain reaction, such that other factors may be involved in the process.

On the basis of the kinetic analyses, the mechanisms that occur through unsubstituted aromatic positions proceed more rapidly, and in general, the retro-ene fragmentation reaction is dominant.

ASSOCIATED CONTENT

Ⓢ Supporting Information

Cartesian coordinates of structures and graphs of steady-state approximation calculations. This material is available free of charge via the Internet at http://pubs.acs.org.

AUTHOR INFORMATION

Corresponding Author

*E-mail: telder@fs.fed.us.

Notes

The authors declare no competing financial interest.

ACKNOWLEDGMENTS

Thomas Elder acknowledges the support of Dr. David C. Young and the Alabama Supercomputer Authority in the performance of this work and Dr. Raymond Fort, Jr. for helpful discussions.

REFERENCES

(1) Menon, V.; Rao, M. *Prog. Energy Combust. Sci.* **2012**, *38*, 522–550.

(2) Demibras, A. *Energy Convers. Manage.* **2009**, *50*, 2872–2801.

(3) Haro, P.; Ollero, P.; Villanueva, A.; Vidal-Barrero, F. *Biofuels, Bioprod. Biorefin.* **2013**, *7*, 551–572.

(4) Pandey, M.; Kim, C. *Chem. Eng. Technol.* **2011**, *34*, 29–41.

(5) Asmadi, M.; Kawamoto, H.; Saka, S. *J. Wood. Sci.* **2010**, *56*, 319–330.

(6) Kotake, T.; Kawamoto, H.; Saka, S. *J. Anal. Appl. Pyrolysis* **2014**, *105*, 309–316.

(7) Asmadi, M.; Kawamoto, H.; Saka, S. *J. Anal. Appl. Pyrolysis* **2011**, *92*, 88–98.

(8) Kawamoto, H.; Horigoshi, S.; Saka, S. *J. Wood Sci.* **2007**, *53*, 168–174.

(9) Brežný, R.; Mihalov, V.; Kováčik, V. *Holzforschung* **1983**, *37*, 199–204.

(10) Holmelid, B.; Kleinert, M.; Barth, T. *J. Anal. Appl. Pyrolysis* **2012**, *98*, 37–44.

(11) Chu, S.; Subrahmanyam, A.; Huber, G. *Green Chem.* **2013**, *15*, 125–136.

(12) Liu, J.-Y.; Wu, S.-B.; Lou, R. *BioResources* **2011**, *6*, 1079–1093.

(13) Brežný, R.; Šurina, I.; Košik, M. *Holzforschung* **1984**, *38*, 19–24.

(14) Britt, P.; Buchanan, A., III; Cooney, M.; Martineau, D. *J. Org. Chem.* **2000**, *65*, 1376–1389.

(15) Britt, P.; Kidder, M.; Buchanan, A., III *Energy Fuels* **2007**, *21*, 3102–3108.

(16) Klein, M.; Virk, P. *Ind. Eng. Chem. Fundam.* **1983**, *22*, 35–45.

(17) Jarvis, M.; Daily, J.; Castensen, H.-H.; Dean, A.; Sharma, S.; Dayton, D.; Robichaud, D.; Nimlos, M. *J. Phys. Chem. A* **2011**, *115*, 428–438.

(18) Huang, X.; Liu, C.; Huang, J.; Li, H. *Comput. Theor. Chem.* **2011**, *976*, 51–59.

(19) Beste, A.; Buchanan, A., III *J. Org. Chem.* **2009**, *74*, 2837–2841.

(20) Wang, H.; Zhao, Y.; Wang, C.; Fu, Y.; Guo, Q. *Acta Chim. Sin.* **2009**, *67*, 893–900.

(21) Elder, T. *Holzforschung* **2010**, *64*, 435–440.

(22) Younker, J.; Beste, A.; Buchanan, A., III *ChemPhysChem* **2011**, *12*, 3556–3565.

(23) Kim, S.; Chmely, S.; Nimlos, M.; Bomble, Y.; Foust, T.; Paton, R.; Beckham, G. *J. Phys. Chem. Lett.* **2011**, *2*, 2846–2852.

(24) Parthasarathi, R.; Romero, R.; Redondo, A.; Gnanakaran, S. *J. Phys. Chem. Lett.* **2011**, *2*, 2260–2666.

(25) Younker, J.; Beste, A.; Buchanan, A., III *Chem. Phys. Lett.* **2012**, *545*, 100–106.

(26) Elder, T. *Energy Fuels* **2013**, *27*, 4785–4790.

(27) Gardrat, C.; Ruggiero, R.; Rayez, M.-T.; Rayez, J.-C.; Castellan, A. *Wood Sci. Technol.* **2013**, *47*, 27–41.

(28) Elder, T. *Energy Fuels* **2014**, *28*, 1175–1182.

(29) Beste, A.; Buchanan, A., III; Britt, P.; Hathorn, B.; Harrison, R. *J. Phys. Chem. A* **2007**, *111*, 12118–12126.

(30) Beste, A.; Buchanan, A., III; Harrison, R. *J. Phys. Chem. A* **2008**, *112*, 4982–4988.

(31) Beste, A.; Buchanan, A., III *Energy Fuels* **2010**, *24*, 2857–2867.

(32) Beste, A.; Buchanan, A., III *J. Org. Chem.* **2011**, *76*, 2195–2203.

(33) Beste, A.; Buchanan, A., III *Chem. Phys. Lett.* **2012**, *550*, 19–24.

(34) Beste, A.; Buchanan, A., III *J. Phys. Chem. A* **2012**, *116*, 12242–12248.

(35) Beste, A.; Buchanan, A., III *J. Phys. Chem. A* **2013**, *117*, 3235–3242.

(36) Moreno, B.; Quach, A.; Merves, M.; Klein, M. *Energy Fuels* **2014**, *28*, 4256–4259.

(37) Stomberg, R.; Lundquist, K. *Nord. Pulp Pap. Res. J.* **1994**, *9*, 37−43.

(38) Frisch, M. J.; Trucks, G. W.; Schlegel, H. B.; Scuseria, G. E.; Robb, M. A.; Cheeseman, J. R.; Scalmani, G.; Barone, V.; Mennucci, B.; Petersson, G. A.; Nakatsuji, H.; Caricato, M.; Li, X.; Hratchian, H. P.; Izmaylov, A. F.; Bloino, J.; Zheng, G.; Sonnenberg, J. L.; Hada, M.; Ehara, M.; Toyota, K.; Fukuda, R.; Hasegawa, J.; Ishida, M.; Nakajima, T.; Honda, Y.; Kitao, O.; Nakai, H.; Vreven, T.; Montgomery, J. A., Jr.; Peralta, J. E.; Ogliaro, F.; Bearpark, M.; Heyd, J. J.; Brothers, E.; Kudin, K. N.; Staroverov, V. N.; Keith, T.; Kobayashi, R.; Normand, J.; Raghavachari, K.; Rendell, A.; Burant, J. C.; Iyengar, S. S.; Tomasi, J.; Cossi, M.; Rega, N.; Millam, J. M.; Klene, M.; Knox, J. E.; Cross, J. B.; Bakken, V.; Adamo, C.; Jaramillo, J.; Gomperts, R.; Stratmann, R. E.; Yazyev, O.; Austin, A. J.; Cammi, R.; Pomelli, C.; Ochterski, J. W.; Martin, R. L.; Morokuma, K.; Zakrzewski, V. G.; Voth, G. A.; Salvador, P.; Dannenberg, J. J.; Dapprich, S.; Daniels, A. D.; Farkas, O.; Foresman, J. B.; Ortiz, J. V.; Cioslowski, J.; Fox, D. J. *Gaussian 09, Revision C.01*; Gaussian, Inc.: Wallingford, CT, 2010.

(39) Zhao, Y.; Truhlar, D. G. *Acc. Chem. Res.* **2008**, *41*, 157−167.

(40) Wiznor, D. J.; Jackson, C.M. J. *J. Mol. Recognit.* **2006**, *19*, 389−407.

(41) Lowry, T. H.; Richardson, K. S. *Mechanism and Theory in Organic Chemistry*; Harper and Row: New York, 1976; p 119.

(42) Jensen, F. *Introduction to Computational Chemistry*; John Wiley and Sons: Chichester, U.K., 1999; pp 297−299.

(43) Sturgeon, M. R.; Kim, S.; Lawrence, K.; Paton, R. S.; Chmely, S. C.; Nimlos, M.; Foust, T. D.; Beckham, G. T. *ACS Sustainable Chem. Eng.* **2014**, *2*, 472−485.